# Accepted Manuscript


Tuning of the Electrochemical Properties of Transparent Fluorine-doped Tin Oxide Electrodes by Microwave Pulsed-plasma Polymerized Allylamine

Anna Cirocka, Dorota Zarzeczańska, Anna Wcisło, Jacek Ryl, Robert Bogdanowicz, Birgit Finke, Tadeusz Ossowski

| | |
|---|---|
| PII: | S0013-4686(19)30968-5 |
| DOI: | 10.1016/j.electacta.2019.05.046 |
| Reference: | EA 34187 |
| To appear in: | *Electrochimica Acta* |
| Received Date: | 07 January 2019 |
| Accepted Date: | 09 May 2019 |

Please cite this article as: Anna Cirocka, Dorota Zarzeczańska, Anna Wcisło, Jacek Ryl, Robert Bogdanowicz, Birgit Finke, Tadeusz Ossowski, Tuning of the Electrochemical Properties of Transparent Fluorine-doped Tin Oxide Electrodes by Microwave Pulsed-plasma Polymerized Allylamine, *Electrochimica Acta* (2019), doi: 10.1016/j.electacta.2019.05.046

This is a PDF file of an unedited manuscript that has been accepted for publication. As a service to our customers we are providing this early version of the manuscript. The manuscript will undergo copyediting, typesetting, and review of the resulting proof before it is published in its final form. Please note that during the production process errors may be discovered which could affect the content, and all legal disclaimers that apply to the journal pertain.

ACCEPTED MANUSCRIPT

# Tuning of the Electrochemical Properties of Transparent Fluorine-doped Tin Oxide Electrodes by Microwave Pulsed-plasma Polymerized Allylamine

*Anna Cirocka[1], Dorota Zarzeczańska[1], Anna Wcisło[1*], Jacek Ryl[2], Robert Bogdanowicz[3], Birgit Finke[4], Tadeusz Ossowski[1*]*

*[1]Department of Analytical Chemistry, Faculty of Chemistry, University of Gdansk, Wita Stwosza 63, 80-308 Gdansk, Poland*

*[2] Department of Electrochemistry, Corrosion and Materials Engineering, Gdansk University of Technology, 11/12 Narutowicza Str.,80-233 Gdansk, Poland*

*[3]Department of Metrology and Optoelectronics, Gdansk University of Technology, 11/12 G. Narutowicza Str., 80-233 Gdansk, Poland*

*[4]Leibniz Institute for Plasma Science and Technology (INP), Felix-Hausdorff-Str. 2, 17489 Greifswald, Germany*

*Corresponding author: anna.wcislo@ug.edu.pl, +48 58 523 5456; tadeusz.ossowski@ug.edu.pl, +48 58 523 5107

**Keywords:** fluorine-doped tin oxide electrodes, surface modification, plasma polymerization, allylamine, direct surface amination,

ACCEPTED MANUSCRIPT

MOST WIEDZY Downloaded from mostwiedzy.pl

## Graphical Abstract

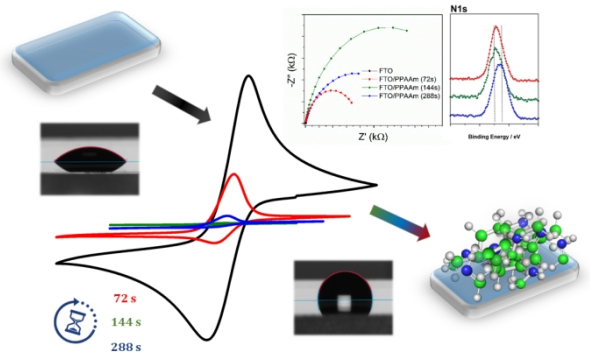


## Abstract

We report here the dry, one-step, and low-temperature modification of FTO surfaces using pulsed plasma polymerization of allylamine (PPAAm). PPAAm/FTO surfaces were characterized by X-ray photoelectron spectroscopy, spectroscopic ellipsometry, and contact angles to understand the morphological, structural, and optical properties. FTO were coated with a very thin layer of adherent cross-linked, pinhole-, and additive-free allylamine plasma polymer resistant to hydrolysis and delamination, and characterized by a high density of positively charged amino groups. Electrochemical studies revealed that PPAAm/FTO electrodes show wide range pH stability and reaction rates tuned by the duration of plasma treatment. We show how the modification of plasma treatment duration between 72 s and 288 s affects the chemical structure and thickness of the obtained modification, having a strong influence on the charge transfer kinetics. In particular, XPS revealed the occurrence of the reduction processes under long-term plasma exposure proving the need for monitoring of this key factor. This covalent immobilization of amine compounds on FTO surface using rapid process in microwave pulsed-plasma makes it a promising electrode for future applications in electrochemical biosensors and optoelectronic devices.

ACCEPTED MANUSCRIPT

MOST WIEDZY Downloaded from mostwiedzy.pl

ACCEPTED MANUSCRIPT

## 1. INTRODUCTION

In recent years, there has been a rapid growth of interest in functional organic polymers. Plasma polymerization is an attractive method for the synthesis of thin organic layers often referred to as "plasma polymer films" (PPF).[1–4] A special feature of this process is that the films can be deposited on any substrate (e.g. polymers, metals, glass, ceramics, silica) with the good adhesion to the substrate. These layers are characterized by the unique physicochemical properties (high thermal and chemical resistance) and are generally highly cross-linked and free from pores.[5] Their most desirable form are homogeneous, defect-free layers. In addition, this technique is more favorable due to the reduced time requirements. Coatings obtained by plasma polymerization find a wide range of applications in the production of biomedical materials or in microelectronics.[6]

Over the past few years, this technique has shown a strong potential to modify the surface properties of various electrode materials.[7–10] The fluorine-doped tin oxide (FTO) electrodes have been recognized as a very promising material due to the stability under atmospheric conditions and the resistance to high temperature. Moreover, this material is chemically inert, mechanically resistant, and has high tolerance to physical abrasion. FTO glass plate is used as a platform (starting material) for the development of electrodes which can act as chemical sensors, due to unique electrochemical and optical properties of the material.[11]

There are only few reports in the literature about obtaining of such structures on the surface of functionalized glass electrodes.[12,13] Optical glasses coated with a layer of conductive inorganic materials ($In_2O_3/SnO_2$, $SnO_2/F$) are an ideal substrate for the modification of their surface properties. A key feature of this type of electrodes is the combination of their optical and electrochemical properties.[14,15] This dualistic nature makes them a potential substrate for the development of optoelectronic sensors. The organic layer present on the surface of the electrode is a precursor for further incorporation of other molecules into the surface structure. Additionally, these molecules contain functional moieties capable of highly specific interactions. The aim of the research is to present the capability concerning obtainment of the allylamine on the surface of FTO using CVD method. In addition, we want to present the modification method for FTO glass electrodes, allowing to record processes of redox-active species, a basis for the molecular recognition systems construction. In our case, different PPAAm film thicknesses were tested and their influence on the electrochemical properties had to be analyzed. Furthermore, we were interested in the following aspects: physico- and



MOST WIEDZY Downloaded from mostwiedzy.pl

electrochemical properties of the deposited film and the influence of various film thicknesses, hydrophilic/hydrophobic properties, acid-base properties, and the ability to carry electrons.

## 2. EXPERIMENTAL METHODS

### 2.1. Cleaning and Pre-treatment Procedures of FTO Electrodes

An important precondition for the subsequent modification steps is a homogeneous chemical clean FTO electrode. Electrodes used as substrates were sequentially sonicated in acetone, ethanol, and ultrapure water for 5 min and dried for 60 min at 70°C prior to immersion in the alkaline piranha solution (RCA solution).[16] After this pre-cleaning step, the substrates were dipped into aqueous RCA solution consisting of hydrogen peroxide, liquid ammonia, and water in the ratio of 1:1:5 for about two hours at 60°C. Afterwards, the electrode was washed with copious amounts of deionized (DI) water and dried at 70°C for 30 min. This preparation procedure of the electrodes ensures the removal of organic surface impurities, and simultaneously the formation of surface functional groups, in our case the hydroxyl groups are necessary as coupling points for binding with various functional groups of different compounds.[17–21]

### 2.2. Plasma Polymerization of PPAAm at FTO Electrodes

In order to obtain selective sensors dedicated to various organic or inorganic compounds, the surface of FTO glass was modified by plasma polymerized allylamine to obtain positively charged amino groups (Figure 1). The functionalization of the FTO electrode were carried out using the commercial microwave plasma reactor V55G (Plasma Finish, Germany; V = 60 L, 2.45 GHz) for the deposition of PPAAm films with different thicknesses as a function of the effective treatment time of 72 s, 144 s, 288 s (sum of the plasma on times).[22] The substrates were positioned downstream, 9 cm under the coupling window. First, the specimens were activated by a continuous wave (cw) Ar-plasma (800 W, 50 Pa, 100 mL Ar, 30 s cw), and without breaking the vacuum, coated with the thin layer of PPAAm using a pulsed low pressure microwave discharge plasma (500 W, 50 Pa, duty cycle DC 0.15, total pulse length 2 s, excitation pulse length 300 ms) with the monomer allylamine ($H_2C$=CH-$CH_2$-$NH_2$) (VWR International GmbH, Germany) and Ar as a carrier gas (50 sccm). A liquid handling system allowed exact dosing of allylamine by a calibrated needle valve (0.125 ± 0.009 mL/min).

MOST WIEDZY Downloaded from mostwiedzy.pl

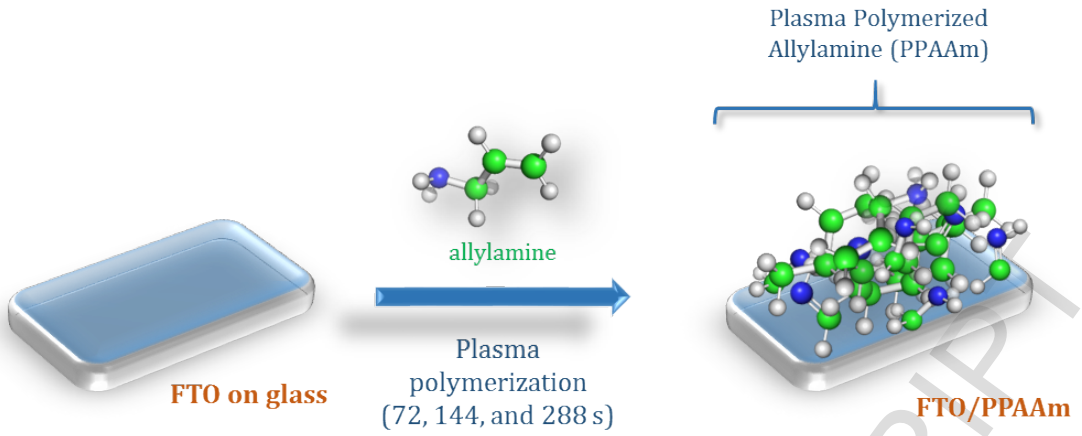


*Figure 1. Scheme of the plasma-polymerized allylamine (PPAAm) functionalization on the FTO electrode surface.*

## 2.3. Instrumentation

### 2.3.1. X-Ray Photoelectron Spectroscopy (XPS)

High-resolution X-Ray Photoelectron Spectroscopy (XPS) analyses were carried out *ex-situ* on FTO functionalized PPAAm samples to evaluate the influence of the plasma polymerization duration on the chemistry of the functionalized film. The spectral analysis was carried out in the binding energy (BE) range characteristic for *C1s*, *O1s,* and *N1s* photopeaks. The studies were carried out using Escalab 250 Xi spectroscope (ThermoFisher, UK) equipped with the monochromatic Al-Kα X-Ray source. The operating parameters were as follows: pass energy 10 eV, energy step size 0.1 eV, X-Ray spot size 250 μm. Charge compensation was controlled by low-energy electron and low-energy $Ar^+$ ions emission using the flood gun (emission current 150 μA, beam voltage 2.1 V, filament current 3.5 A). Spectral deconvolution was performed using Avantage software provided by the manufacturer.

### 2.3.2. Cyclic Voltammetry (CV)

Cyclic voltammetry (CV) measurements were carried out in aqueous solution of $Na_2SO_4$ (0.5 M) containing reference redox system of $[Fe(CN)_6]^{3-/4-}$ (5 mM) and in non-aqueous solution (DMF) containing ferrocene/ferrocenium (5 mM) in 0.1 M tetrabutylammonium perchlorate (TBAP) (Supporting information). Measurements performed in the aqueous solution were recorded in phosphate buffer solutions (pH = 2.15, 3.61, 7.43, 9.17) in a three-electrode system. The buffered solutions were prepared according to the procedure described in European Pharmacopeia 7.0. In addition, the pH of the prepared solutions was



MOST WIEDZY Downloaded from mostwiedzy.pl

measured each time using a Schott Blue line N16 pH electrode.[23] FTO electrode (modified or unmodified) were used as the working electrode. An Ag/AgCl (0.1M KCl) and platinum wires were used as the reference and counter electrodes, respectively. The area of the working electrode exposed to the electrolyte was approximately 0.5 $cm^2$. All cyclic voltammograms were scanned at 100 mV/s. The electrochemical experiments were performed using Autolab potentiostat/galvanostat PGSTAT30 and Nova 1.11 (Metrohm Autolab B.V) software.

### 2.3.3. Electrochemical Impedance Spectroscopy (EIS)

The electrochemical impedance spectroscopy (EIS) measurements were performed at the rate of 40 points per decade between 10 kHz to 100 mHz with a 10 mV amplitude of the AC signal. Measurements were performed at the open circuit potential (OCP values = 0.140 V) using the same aqueous solution of CVs measurement.

### 2.3.4. Contact Angle Measurements (CA)

Wetting properties of FTO modified and unmodified electrodes were studied using the contact angle measurement and were carried out at room temperature using water based on the static sessile drop method. The reported contact angle values were the average values measured at five different positions of the electrode surfaces. The drop shape analysis was conducted using circle and Young-Laplace method with 2 µl of water.[24–26] These measurements were performed using KRÜSS Drop Shape Analyzer – DSA100 equipment.

### 2.3.5. Spectroscopic Ellipsometry

Spectroscopic ellipsometry investigations were carried out with a phase-modulated ellipsometer Jobin-Yvon UVISEL (HORIBA Jobin-Yvon Inc., Edison, USA) to estimate the PPAAm film thickness and quantify its structure. As ellipsometry is sensitive to differences in the optical density between the adsorbate and the bulk solution, it essentially senses the adsorbate mass.[27] The PPAAm were simultaneously deposited on the reference Si wafers to simplify the optical model and avoid depolarization effects. Nevertheless, the reference Si samples undergo the same pre-treatment and growth procedure as FTO ones. The SE was carried out at the wavelength region of 250–800 nm with a step of less than 0.5 nm. The experiments were performed at the room temperature using an angle of incidence fixed at 70° and the compensator was set at 45°. DeltaPsi software (v. 2.4.3) was employed to determine the thickness and optical constants of the PPAAm films. A four-layer structural model



MOST WIEDZY Downloaded from mostwiedzy.pl

(ambient/PPAAm/native oxide/Si-wafer) was applied to the samples to determine the thickness of PPAAm film and its optical constants, respectively. We have conducted three independent measurements in the three different points at the middle area of samples to avoid edge effects. The optioned ellipsometric angles were averaged. Next, the thickness of the deposited plasma polymer film was measured with the surface profiler Dektak3ST′ (Veeco, USA). These values were applied for the ellipsometric studies as a starting point in the fitting process resulting in the low mean square error. The PPAAm film was simulated as a transparent and homogeneous material and its dispersion was fitted to the single classical oscillator model with Drude component.[28] The optical model was fitted to the experimental data using the non-linear Levenberg-Marquardt regression method and the mean-square error of minimization (MSE).[29]

## 3. RESULTS AND DISCUSSION

### 3.1. Electrochemical Performance of FTO/PPAAm Electrodes

Firstly, our goal was to distinguish whether the modification with the chemical vapor deposition method occurred and to describe the properties of the obtained layer. A clear evidence of the modification process effectiveness is particularly the change in the electrochemical properties of the electrode: the observed resistance in the charge transfer at the surface of the electrode. We used the electrochemical impedance spectroscopy (EIS) for this purpose.

ACCEPTED MANUSCRIPT

MOST WIEDZY Downloaded from mostwiedzy.pl

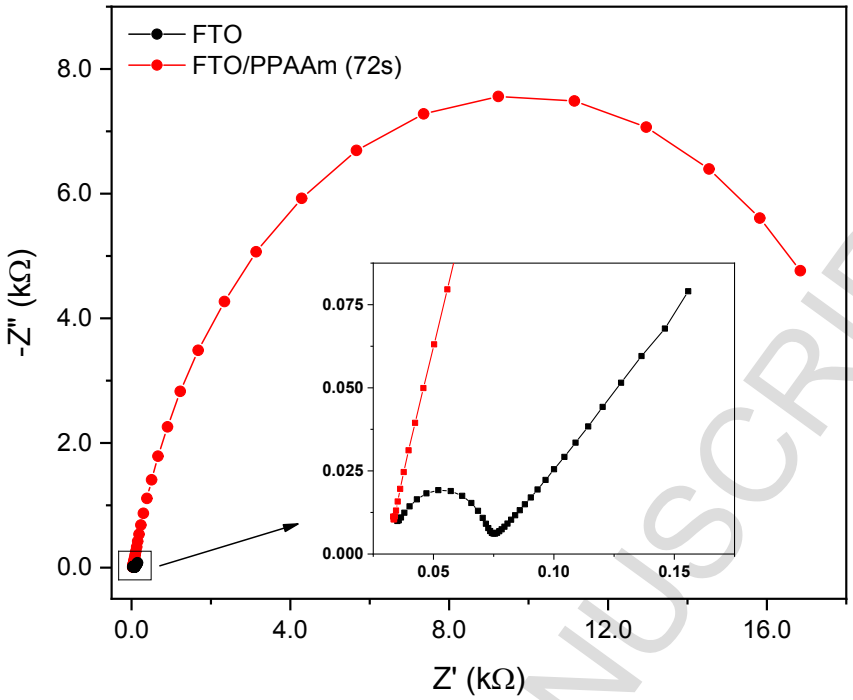


*Figure 2. Nyquist plots obtained for unmodified FTO glass and FTO glass electrode after direct surface amination (72 s) in 0.5 M KCl solution containing 5 mM $[Fe(CN)_6]^{3-/4-}$.*

EIS spectra shown on (Figure 2) reveal how modification with PPAAm film affects the charge transfer process on FTO electrode. The unmodified electrode is characterized by high kinetics, charge transfer resistance $R_{CT}$ value was approximated based on a spectra shape as ~45 Ω.[30] The inclined line at low frequencies indicates diffusion control of the electrochemical process.[31–33] On the other hand, the modification with PPAAm leads to the decrease in the kinetics of the electron transfer, which lowers the reversibility of the charge transfer process. The $R_{CT}$ of FTO/PPAAm (72 s) electrode was ~20.2 kΩ. Due to the significant differences in the shape of the impedance spectra, the electric equivalent circuits were not used for the direct comparison of the impedance results.

Both the impedance spectroscopy and the cyclic voltammetry are the techniques that enable the characterization of the conductive material surface properties. Furthermore, it is possible to control the modification process based on the observation of changes in the charge transfer processes — resistance and conductivity reflect the changes in the character of the surface structure. As a result of the modification, a significant increase in the charge transfer resistance



MOST WIEDZY Downloaded from mostwiedzy.pl

was observed, what indicates a difficulties in the electron transport within the modified FTO electrode surface. These results are compatible with the measurements obtained for the cyclic voltammetry.

Both KCl and $Na_2SO_4$ were used as a supporting electrolyte. The figures 2–7 were selected to illustrate the phenomena presented in this work, to highlight the discussed changes, and to clarify the given problem.

The deposited PPAAm layer on the surface of the FTO electrode is a barrier to the $[Fe(CN)_6]^{3-/4-}$ system — the electron transfer is difficult. We observe a significant reduction in the value of current responses and the lack of the redox process reversibility for the amine-containing structure of FTO electrode in an aqueous solution. In the case of the modified electrode, the potential of the redox process changed to 0.074 V from 0.158 V. Therefore, we can conclude that the reversibility of the process is improved after modification. The cathodic current decreased from -52.2 μA to -8.62 μA compared to unmodified FTO — similar behavior was observed for the anodic current. The PPAAm layer formed as a result of allylamine deposition on the surface of the electrode should exhibit hydrophobic properties which can cause poor electron and ion penetration in the case of an aqueous solution.

ACCEPTED MANUSCRIPT

MOST WIEDZY Downloaded from mostwiedzy.pl

*Table 1. Electrochemical parameters (with standard deviation) of the reference redox system in an aqueous ($Na_2SO_4$) solution on the unmodified and modified FTO glass electrode.*

| Type of electrode | Redox system | $E_a$ (V) | $E_c$ (V) | ΔE (V) | $E_f$[a] (V) | $I_a$ (μA) | $I_c$ (μA) | $\|I_c/ I_a\|$ |
|---|---|---|---|---|---|---|---|---|
| FTO | $[Fe(CN)_6]^{3-/4-}$ | 0.221 (±0.002) | 0.063 (±0.002) | 0.158 | 0.142 | 66.7 (±0.25) | -52.2 (±1.05) | 0.78 |
| FTO/PPAAm (72 s) | $[Fe(CN)_6]^{3-/4-}$ | 0.165 (±0.002) | 0.091 (±0.038) | 0.074 | 0.128 | 22.4 (±0.17) | -8.62 (±0.88) | 0.38 |

[a] $E_f = (E_a + E_c)/2$.

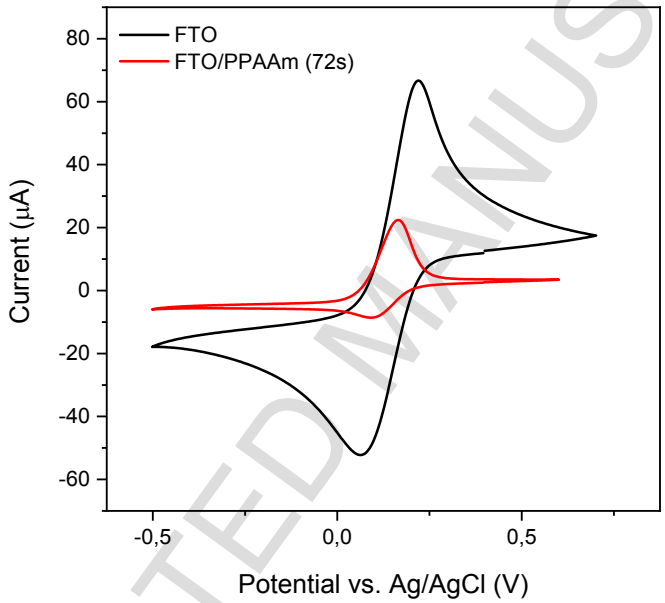


*Figure 3. Cyclic voltammograms of unmodified FTO glass and the FTO glass electrode after direct surface amination (72 s) in the aqueous solution of 5 mM $[Fe(CN)_6]^{3-/4-}$ in 0.5 M $Na_2SO_4$; scan rate 100 $mVs^{-1}$.*

It is known that the acid-base reactions are crucial for both organic and inorganic chemistry. Ferri-/ferrocyanide redox probe is recognized as a pH-sensitive redox couple. In strong alkaline pH, where the concentration of $OH^-$ ions is high. Hydroxyl ion can act as a strong nucleophile and attack the electrophilic redox active species, which can lead to an irreversible chemical decomposition.[34] Therefore, this redox couple exhibits the weakest electrochemical performance under strong alkaline conditions and under weak alkaline conditions. Additionally, this performance is altered by the properties of the surface (due to the changes after modification). This phenomenon is observed in the case of the unmodified FTO electrode over



MOST WIEDZY Downloaded from mostwiedzy.pl

pH 7 (Figure 4a). For a modified FTO electrode, both the reversibility and the currents of the redox processes are already decreasing at pH 3.61. No anodic response was recorded for neutral and alkaline pH.

Ferri-/ferrocyanide is a quasi-ideal inner sphere redox couple and its kinetics are sensitive to many factors, such as surface pretreatment. The pH change of the water solution has a significant impact on the redox processes. The presence of positively charged groups on the surface of the electrode may alter the electrochemical performance of this negatively charged redox probe. The protonation of amino groups occurs in the acidic environment — the surface is positively charged and thus electrostatic interactions with negatively charged redox species ($[Fe(CN)_6]^{3-/4-}$) occur. Hence, the efficiency of the electron transfer increases. The transfer of electrons through the double layer is enhanced and we obtain a better current response while improving the peak-to-peak separation. Moreover, the unequal cathodic and anodic peak currents are the further confirmation of the quasi-reversibility/irreversibility of the redox process.

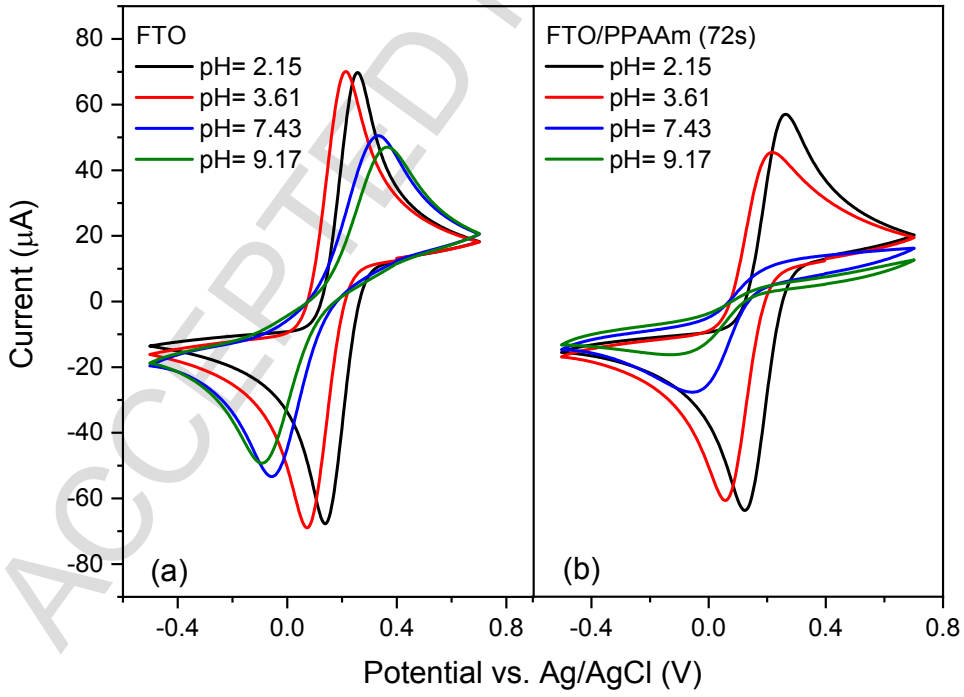


*Figure 4 Cyclic voltammograms of 5 mM $[Fe(CN)_6]^{3-/4-}$ recorded at various pH values for: (a) unmodified FTO glass electrode and (b) the FTO glass electrode after direct surface amination (72 s) in 0.5 M $Na_2SO_4$, scan rate 100 $mVs^{-1}$.*



MOST WIEDZY Downloaded from mostwiedzy.pl

### 3.2. Studies on the Composition of PPAAm Films Grown at FTO

If the electrode surface is covered with an PPAAm layer, it should be more hydrophobic than the FTO oxide layer. The contact angle measurements of the modified electrodes were made to confirm the effectiveness of the modification. The plasma deposition of allylamine on the surface significantly changes the contact angle. The oxidized FTO electrode is highly hydrophilic and reaches the angles of 45.25°.[35,36] The obtained modified FTO/PPAAm (72 s) electrodes are characterized by a wetting angle of 90.97° (Figure 8, Table 3). These results confirm the hydrophobicity of the surface and thus support the effectiveness of the modification.

The XPS analysis of the unmodified FTO sample reveal the chemical composition often reported in similar materials. Detailed analysis of *O1s* energy range reveals three primary types of oxygen chemical states (Figure 5). The peak deconvoluted as $O_{FTO}$ owing the lowest binding energy corresponds to the $O^{2-}$ state forming [$SnO_6$] octahedrons with adjacent $Sn^{4+}$ in the $SnO_2$ lattice, while the second component, marked as $O_{FTO}$* and shifted by +1.1 eV, corresponds to non-stoichiometric oxygen which fails to form [$SnO_6$] octahedrons. The third and least significant component is related to the hydroxyl groups or adsorbed oxygen on the particle surface.[37–39] The amount of carbon contribution observed as *C1s* photopeak does not exceed 10 at.% and originates from the storage in the atmospheric air. The adventitious carbon is typically observed at 284.6 eV, asin this case.[40,41]

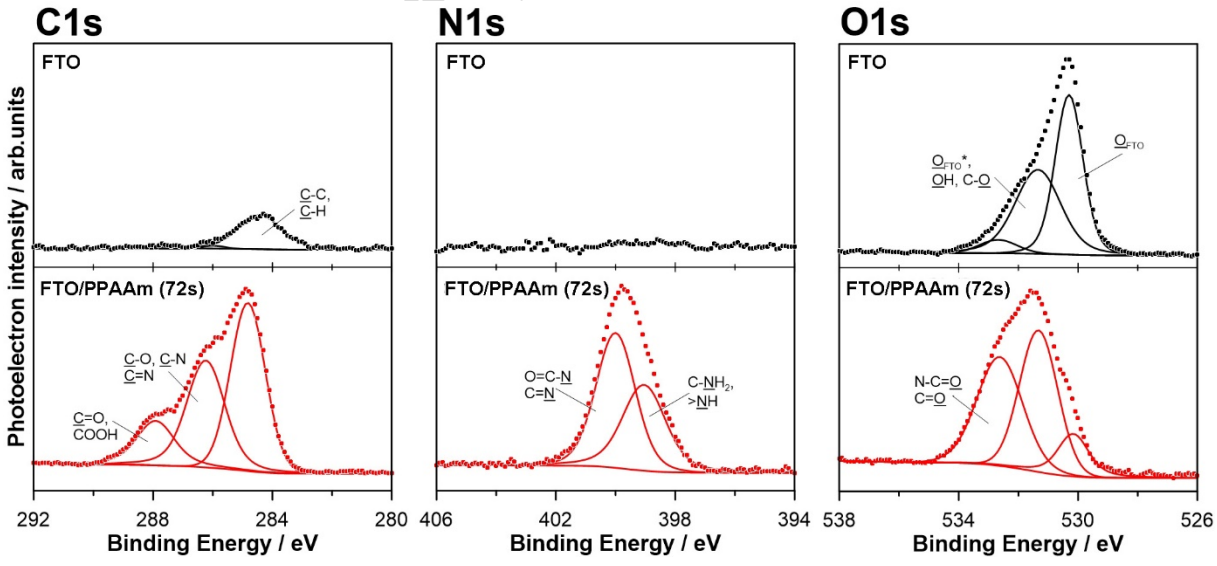


*Figure 5. High-resolution XPS spectra in the energy range of C1s, N1s, and O1s photopeaks with spectral deconvolution for FTO (top) and FTO/PPAAm (72 s, below).*



MOST WIEDZY Downloaded from mostwiedzy.pl

XPS deconvolution conducted to determine the surface chemical composition of the PPAAm coating revealed greatly enhanced surface chemistry. There are numerous carbon chemical states overlapping on the XPS spectra, thus a simplified deconvolution model has been proposed. Spectra recorded in *C1s* energy range reveal the dominant presence of the component at approx. 284.6 eV, which corresponds to the aliphatic C-C and C-H bonds in the plasma-polymerized film. The second, most notable component, shifted approx. +1.4 eV should be ascribed to C-O bonds but also C-N bonds in both amine and imine functional groups [10,42,43]. More positive energy shift, between +3.1 to even +4.0 eV, is the characteristic feature for carbonyl and carboxyl groups.

The *N1s* photopeak was fitted as a combination of two primary components. The most notable is the component present at 400.0 eV and related with O=C-N and C=N bonds, while second component shifted to more negative BE values represents primary and secondary amine groups.[42–45]

XPS analysis also revealed oxygen incorporation into the coating due to the non-ultra-high-vacuum conditions. The oxygen chemistry was confirmed by fitted *O1s* peaks. The broad and prominent peak located at 532.6 eV most likely corresponds to the previously reported amide and carbonyl groups. The second notable component at 531.3 eV derives from hydroxyl and ester bonds, resulting from the air contamination among other things. The last and small contribution comes from the FTO base due to the small thickness of the analyzed PPAAm film. Thus, it is possible to estimate its diverse thickness, which does not exceed 10 nm for modified FTO sample (72 s).

### 3.3. Tuning Properties of FTO/PPAAm Electrodes by Polymerization Time

As it has been shown in the literature,[9,10] an important factor in the plasma modification process is the duration of the deposition process. In order to optimize this factor, the FTO electrodes were modified using three times: 72 s, 144 s, 288 s. Physicochemical studies showed differences in the properties, film thickness, and structure of the resulting layers.

It would seem that the prolongation of the allylamine deposition time will increase the thickness of the modified layer, thus hindering the electrode processes. However, analysis of Nyquist plots showed that the greatest resistance is observed in the case of the 144 s electrode (Figure



MOST WIEDZY Downloaded from mostwiedzy.pl

6), i.e. the electrode with the intermediate deposition time. Similarly, the results obtained by the cyclic voltammetry method were not predictable. Extending the deposition process reduced the peak currents and kinetics of the processes occurring on the electrode 144 s to 72 s in contrast to the 288 s electrode, for which these parameters (peak currents and kinetics of redox process) were more favorable than the previous ones.

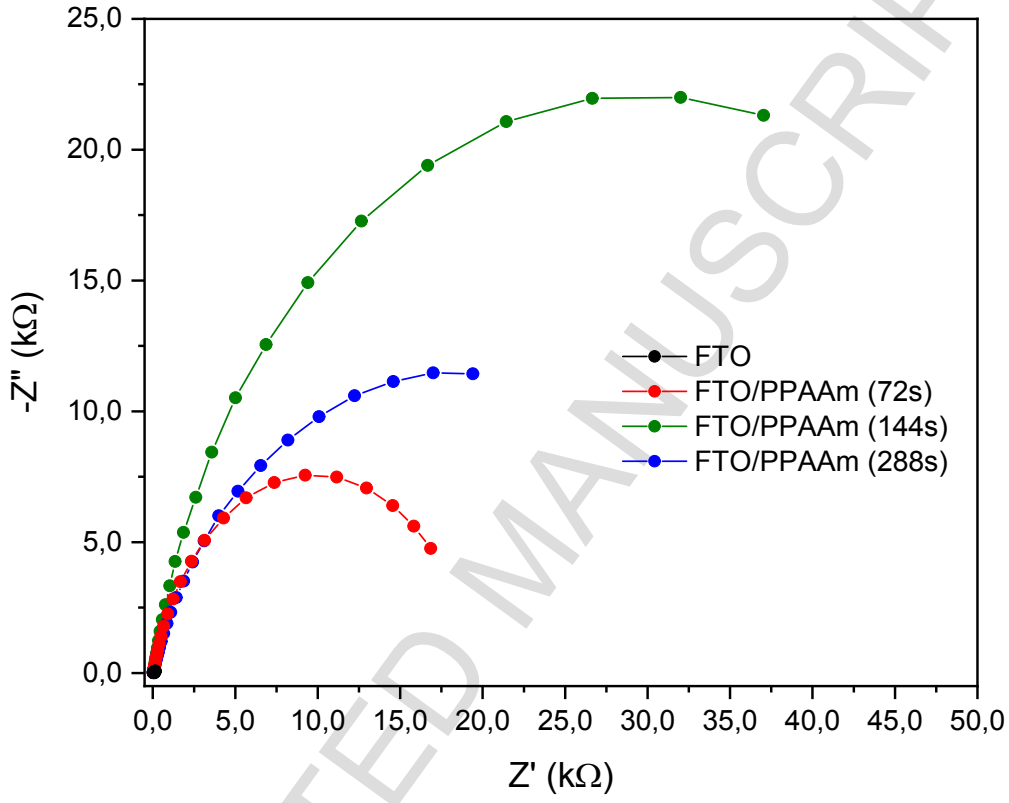


*Figure 6. Nyquist plots obtained for unmodified FTO glass and the FTO glass electrode after direct surface amination with various deposition times (72 s, 144 s, 288 s) in 0.5 M KCl solution containing 5 mM $[Fe(CN)_6]^{3-/4-}$.*

In order to provide more detailed information on the base of EIS studies, it is essential to propose an electric equivalent circuit (EEC), efficiently representing the electrode-electrolyte interface. A Randless circuit was selected for this purpose, since the impedance spectra composed of a singular time constant. Furthermore, the capacitor was replaced with the constant phase element (CPE) to take into consideration the normal distribution of the time constants due to heterogeneous electric properties from various parts of PPAAm layer. The CPE impedance $Z_{CPE} = (Q(j\omega)^n)^{-1}$, where Q represents quasi-capacitance in case of time-constant dispersion and n is the heterogeneity factor. For homogeneous surface n=1 and CPE represents



MOST WIEDZY Downloaded from mostwiedzy.pl

a capacitor with capacitance 1/Q.[40,46–48] Aforementioned solution was proposed to take into account the significantly altered chemical composition between the polymerized electrodes, as demonstrated further in the manuscript based on the XPS studies. The effective capacitance of the double-layer $C_{eff}$ can be calculated based on CPE using an algorithm proposed by Hirshorn *et al.*[49] The results of EIS analysis using proposed R(QR) EEC are presented in Table 2.

*Table 2. Electric parameters obtained based on EIS studies from Fig. 7 analyzed using R(QR) EEC and Hirschorn's algorithm for normal distribution of time constants.*

| | Rct / kΩ | Q / μSs$^n$ | n / - | $C_{eff}$ / μF |
|---|---|---|---|---|
| FTO/PPAAm (72 s) | 20.24 | 26.69 | 0.82 | 21.29 |
| FTO/PPAAm (144 s) | 57.02 | 16.77 | 0.84 | 16.63 |
| FTO/PPAAm (288 s) | 29.95 | 27.94 | 0.77 | 26.55 |

$R_{CT}$ analysis confirm the previously stated hypothesis that the highest film thickness was observed after 144 s of FTO polymerization while increased polymerization durations lead to secondary thickness reduction. At the same time, the drop of CPE exponent n reveals a significant increase of PPAAm film heterogeneity as a result of prolonged polymerization time and possible etching effects by plasma. The thickness of the polymerized layer $d_{PPMMa}$ is reversely proportional to the $C_{eff}$ parameter, using the relationship $d_{PPAAm} \cong \frac{\varepsilon_0 \varepsilon A}{C_{eff}}$, where $\varepsilon_0$ is the vacuum permittivity, ε is PPAAm dielectric permittivity, A is the electrode surface area, and d is the film thickness. The same value of ε was assumed for each polymerized film, based on their negligible differences in the ellipsometric studies. Increased time of plasma polymerization effects in higher PPAAm film thickness, manifested by the decrease of $C_{eff}$ value. In the case of FTO/PPAAm (288 s), the high $C_{eff}$ value results from the combined effects of $d_{PPAAm}$ decreased and confirmed electrochemically active surface area A growth, both due to the aforementioned etching effects.

In voltammetric measurements, analogously to the impedimetric measurements, the values of peak currents for the reduction and oxidation reactions of the $[Fe(CN)_6]^{3-/4-}$ system showed a disproportionate dependence on the length of polymerization time (Figure 7). The lowest value of the current was observed in the $Na_2SO_4$ solution for the electrode (144 s). This result indicates the inhibition of the electron transfer process and shows an impact of the modified layer structure on the hindering of the redox process of the ferri-/ferrocyanide couple. Surprisingly high currents are observed for the electrode at 288 s. Based on this finding, we assume that the



MOST WIEDZY Downloaded from mostwiedzy.pl

prolonged polymerization lead to the modification of the outer part of the polymer resulting with such specific properties.

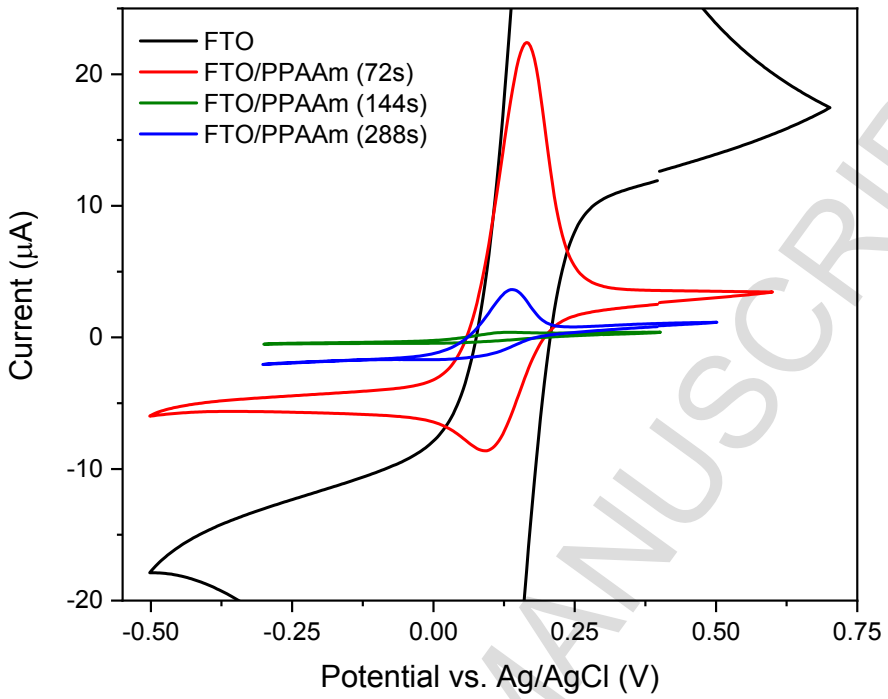


*Figure 7. Cyclic voltammograms of unmodified FTO glass and the FTO glass electrode after direct surface amination (72 s, 144 s, 288 s) in an aqueous solution of 5 mM $[Fe(CN)_6]^{3-/4-}$ in 0.5 M $Na_2SO_4$.*

An increase in the carbon content in the organic layer of the electrode is also visible in the values of the contact angle (Figure 8, Table 3). The most hydrophobic layer was obtained after the modification time of 144 s. The contact angle values for this layer is 92.90°, which is greater than for 288 s (CA= 67.26°), and 72 s (CA= 90.97°). One should remember that these differences are small.

*Table 3. Contact angle measurements of unmodified and modified FTO electrodes.*

| | FTO | FTO/PPAAm (72 s) | FTO/PPAAm (144 s) | FTO/PPAAm (288 s) |
|---|---|---|---|---|
| **CA value** | 45.25°(±0.49) | 90.97° (±0.66) | 92.90°(±0.67) | 67.26°(±0.32) |

ACCEPTED MANUSCRIPT

MOST WIEDZY Downloaded from mostwiedzy.pl

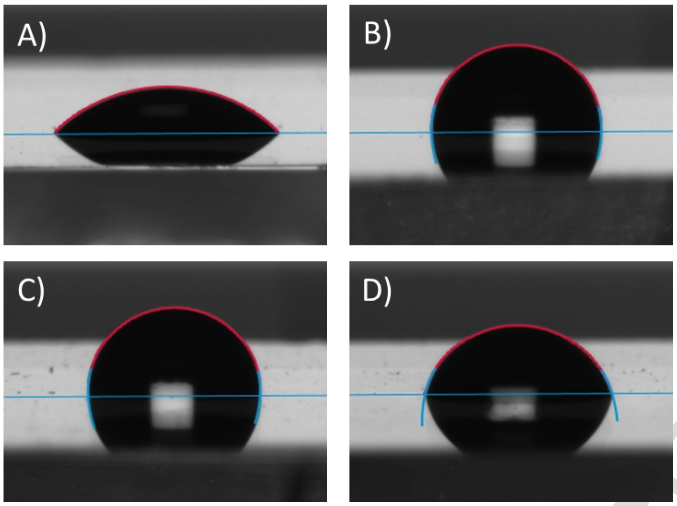


*Figure 8. Contact angle measurement images of (a) unmodified FTO; (b) FTO/PPAAm (72 s), (c) FTO/PPAAm (144 s); (d) FTO/PPAAm (288 s).*

These parameters indicate the diverse structure of the layers. Differences in the hydrophobicity as well as the number and type of nitrogen groups suggest that the deposition-related processes depend on time. An increase in the carbon content and hydrophobicity of the 144 s layer indicates that the elongation of time causes the polymerization with a greater share of allylic radicals. Further prolongation of the deposition time can lead to the etching of the plasma layer which reveals the internal structure of the layer richer in amino groups, thus improving the electrochemical parameters, as well as the wettability of the surface.

High-resolution XPS spectroscopy carried out for electrodes characterized with different durations of PPAAm polymerization are shown in Figure 9. Detailed chemical analysis was carried out using previously proposed deconvolution model — detailed results are summarized in Table 4.

ACCEPTED MANUSCRIPT

MOST WIEDZY Downloaded from mostwiedzy.pl

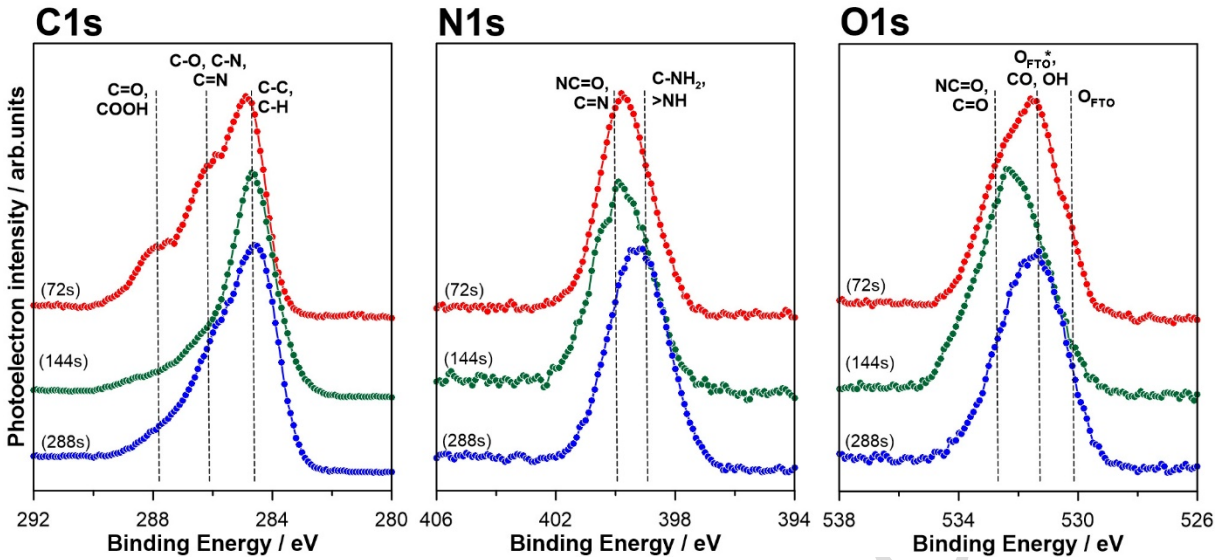


*Figure 9. High-resolution XPS spectra in the energy range of C1s, N1s, and O1s photopeaks for FTO/PPAAm electrodes; modification at various polymerization duration.*

The chemical structure of PPAAm film differs significantly between the electrodes that are characterized by different polymerization durations.

While the most notable *N1s* spectra component for short-time modified FTO samples (72 s, 144 s) is related with O=C-N and C=N bonds, the increase in the polymerization time results in the higher amount of observed amine groups. The relationship between *N1s* peaks intensity suggests the occurrence of the reduction processes under the long-time plasma influence. The above statement finds confirmation in the *C1s* peak analysis, where the highest share of oxidized carbon components is visible for the lowest modification time ($C_{ox}$:$C_{red}$ = 1.1:1, 0.5:1, and 0.6:1, respectively with the increase of the polymerization time). Finally, the surface chemistry after 288 s is highly resembling analogous layers reported for the modification of BDD electrodes.[9]

As expected, the thinnest layer is obtained after 72 s-long PPAAm polymerization process. Here, the $O_{FTO}$ share reaching 15% of *O1s* signal was observed suggesting that the overall layer thickness does not exceed 10 nm. Prolonged polymerization time reduce $O_{FTO}$ signal within deconvoluted spectra to minimum, where it is no longer possible to distinguish the thickness of polymerized film based on the XPS results.

MOST WIEDZY Downloaded from mostwiedzy.pl

*Table 4. Results of the high-resolution XPS spectra deconvolution.*

| | Chemical state | Binding Energy eV | FTO at. % | FTO/PPAAm (72 s) at. % | FTO/PPAAm (144 s) at. % | FTO/PPAAm (288 s) at. % |
|---|---|---|---|---|---|---|
| C1s | C-C, C-H | 284.8 | 9.9 | 32.1 | 50.6 | 43.1 |
| | C-O, C-N, C=N | 286.2 | 0.4 | 24.1 | 20.1 | 20.8 |
| | C=O, COOH | 287.9 | -- | 10.7 | 7.3 | 7.9 |
| O1s | $O_{FTO}$ | 530.2 | 45.2 | 2.3 | 0.4 | 0.9 |
| | $O_{FTO}$*, CO, OH | 531.3 | 40.3 | 8.0 | 3.9 | 5.8 |
| | NC=O, C=O | 532.6 | 4.2 | 7.5 | 7.3 | 3.7 |
| N1s | C-$NH_2$, >NH | 399.1 | -- | 6.5 | 2.4 | 11.7 |
| | NC=O, C=N | 400.0 | -- | 8.8 | 8.0 | 6.1 |

Figure 10 presents the measured ellipsometric psi ($\Psi$) and delta ($\Delta$) angles versus wavelength. The shape of recorded distribution of ellipsometric angles shows standard Si-wafer-like trend in agreement with the nanometre scale of PPAAm thickness and low optical absorption of deposited polymer. The standard Si-wafer reference samples were applied to minimize the influence of FTO on the optical analysis and depolarization effect, while the growth process is not substrate-sensitive in the principle. Both ellipsometric angles are dependent on the properties of analysed PPAAm samples. Nevertheless, $\Delta$ is more sensitive to the thin PPAAm thickness.[29] The lowest $\Delta$ values were recorded for Si(144 s) sample (see Inset: Figure 10B), what is attributed to the highest PPAAm film thickness. The thickness estimated by ellipsometry PPAAm are 1.8±0.1 nm, 12.9±0.4 nm, and 8.3±0.9 nm for 72, 144, and 288 seconds of deposition, respectively. The Si(144 s) sample results also in the highest growth rate of 5.4 nm $min^{-1}$, which is comparable with the previous work of Lejeune *et al.*[50] The 72 and 288 seconds of deposition results in much lower thickness along with growth rates. The nonlinear trend of growth kinetics is attributed first to the polymer nucleation stage of growth (72 seconds) and next to the densification and etching effects for longer times (288 seconds).

ACCEPTED MANUSCRIPT

MOST WIEDZY Downloaded from mostwiedzy.pl

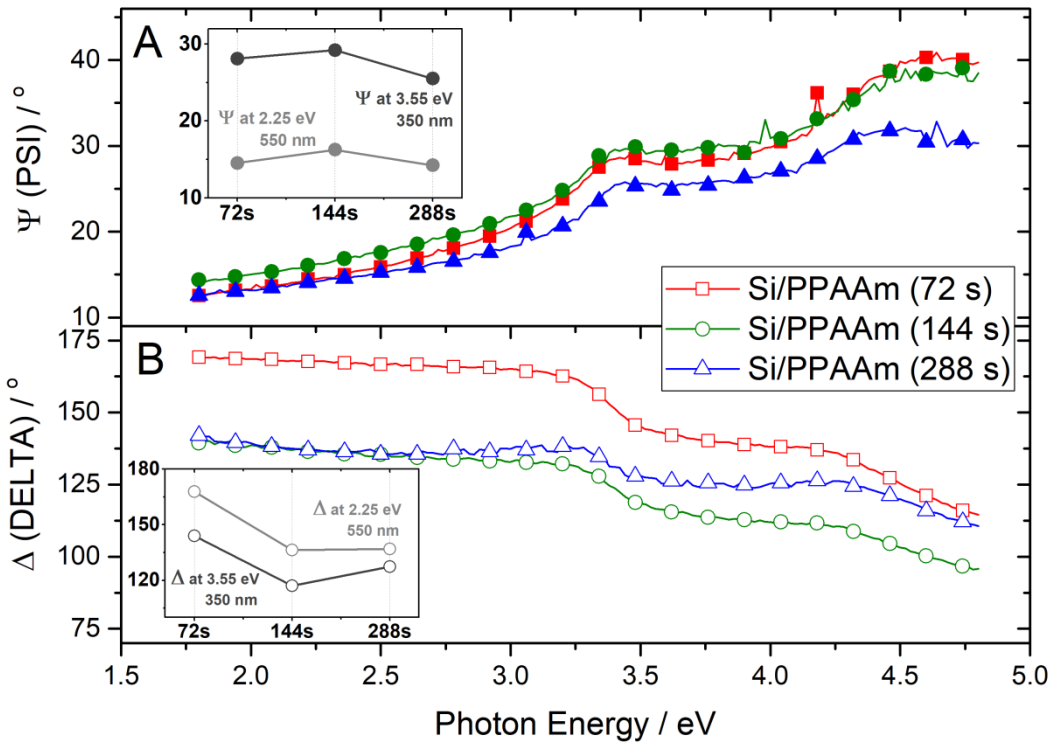


*Figure 10. Spectral dependences of ellipsometric angles Δ(λ) and Ψ(λ) for PPAAm-modified Si reference samples, modification at various polymerization duration. Insets: Variation of Δ(λ) and Ψ(λ) at 2.25 eV (550 nm) and 3.55 eV (350 nm) vs the polymerization time.*

The 288 seconds of deposition delivers the highest refractive index of 1.52 @ 550 nm, when compared with 144 seconds (1.43 @ 550 nm). This effect was manifested in Ψ values. The inset in Figure 10A illustrates the lowest Ψ angles for Si (288 s) sample. The refractive index changes are usually directly related to the amount of molecules present in the deposited layer, though these values could be used for the indirect density assessment. Summarizing, the 144 seconds sample shows the highest thickness, while the 288 seconds results in the highest density. Low optical absorption of samples effects in a similar extinction coefficient of approx. 0.02 @ 550 nm for all the samples. The optical constants estimated herein are in agreement with the previous works of Elzbieciak *et al.*[51] and Schlenoff *et al.*[47] revealing the possible effective utilization of SE for the plasma polymerization process investigation and revealing its dependency to the duration of the deposition.

ACCEPTED MANUSCRIPT

MOST WIEDZY Downloaded from mostwiedzy.pl

## 4. CONCLUSIONS

Our study confirmed the effectiveness of FTO electrodes modification by means of plasma polymerization. The polymerized allylamine layer changes the electrochemical properties of the electrode. The consequence of embedding is the increased resistance of the layer and the decrease in the peak currents of the reduction and oxidation currents of the $[Fe(CN)_6]^{3-/4-}$ system. In an aqueous solution, this system depends on the pH of the solution. Protonation of the amino groups present in the PPAAm film enhances the transfer of electrons through the double layer. Covering the oxide layer with an allylamine polymerization product results in a significant increase in the surface hydrophobicity. XPS showed the presence of C-C and C-H bonds and bonds with nitrogen atoms typical of organic layers. Prolongation of the polymerization changes the layer structure. The increase in the layer thickness occurs only up to 144 s of the deposition. Further plasma exposure results in the decreased thickness associated with the plasma etching. Both electrochemical parameters and wettability of the surface confirm this thesis. At the longest polymerization time, the water contact angle is close to that for the shortest time, as well as the resistance of the layer is similar to that obtained for 72 seconds. XPS measurements also confirm that the chemical structure of the PPAAm film significantly varies between the electrodes with different polymerization time. The relationship between *N1s* peaks intensity suggests the occurrence of the reduction processes under long-time plasma influence. Ellipsometry indicated that the 144 seconds sample showed the highest thickness, while the 288 seconds deposition results in the highest density.

## 5. ACKNOWLEDGMENT

The authors gratefully acknowledge the financial support from the Polish National Science Centre (NCN) under Grant Nos. UMO-2014/14/E/ST7/00104, UMO-2014/14/M/ST5/00715, the National Centre for Science and Development Grant Techmatstrateg No. 347324, and the project supporting young scientists and PhD students No. 538-8210-B730-17/18. The DS funds of the Faculty of Electronics, Telecommunications, and Informatics of the Gdańsk University of Technology are also acknowledged.

MOST WIEDZY Downloaded from mostwiedzy.pl

## 6. REFERENCES


[1] S.W. Myung, H.S. Choi, Chemical structure and surface morphology of plasma polymerized-allylamine film, Korean J. Chem. Eng. 23 (2006) 505–511. doi:10.1007/BF02706757.

[2] L. Denis, D. Cossement, T. Godfroid, F. Renaux, C. Bittencourt, R. Snyders, M. Hecq, Synthesis of Allylamine Plasma Polymer Films: Correlation between Plasma Diagnostic and Film Characteristics, Plasma Process. Polym. 6 (2009) 199–208. doi:10.1002/ppap.200800137.

[3] K. Vasilev, A. Michelmore, H.J. Griesser, R.D. Short, Substrate influence on the initial growth phase of plasma-deposited polymer films, Chem. Commun. 0 (2009) 3600–3602. doi:10.1039/B904367E.

[4] M.T. van Os, B. Menges, R. Foerch, G.J. Vancso, W. Knoll, Characterization of Plasma-Polymerized Allylamine Using Waveguide Mode Spectroscopy, Chem. Mater. 11 (1999) 3252–3257. doi:10.1021/cm991068k.

[5] H. Schönherr, M.T. van Os, R. Förch, R.B. Timmons, W. Knoll, G.J. Vancso, Distributions of Functional Groups in Plasma Polymerized Allylamine Films by Scanning Force Microscopy Using Functionalized Probe Tips, Chem. Mater. 12 (2000) 3689–3694. doi:10.1021/cm0010351.

[6] Q. Chen, R. Förch, W. Knoll, Characterization of Pulsed Plasma Polymerization Allylamine as an Adhesion Layer for DNA Adsorption/Hybridization, Chem. Mater. 16 (2004) 614–620. doi:10.1021/cm034529h.

[7] M. Ardhaoui, S. Bhatt, M. Zheng, D. Dowling, C. Jolivalt, F. Arefi-Khonsari, Biosensor based on laccase immobilized on plasma polymerized allylamine/carbon electrode, Mater. Sci. Eng. C Mater. Biol. Appl. 33 (2013) 3197–3205. doi:10.1016/j.msec.2013.03.052.

[8] M. Wang, S. Liu, Y. Zhang, Y. Yang, Y. Shi, L. He, S. Fang, Z. Zhang, Graphene nanostructures with plasma polymerized allylamine biosensor for selective detection of mercury ions, Sens. Actuators B Chem. Complete (2014) 497–503. doi:10.1016/j.snb.2014.07.009.

[9] R. Bogdanowicz, M. Sawczak, P. Niedzialkowski, P. Zieba, B. Finke, J. Ryl, J. Karczewski, T. Ossowski, Novel Functionalization of Boron-Doped Diamond by Microwave Pulsed-Plasma Polymerized Allylamine Film, J. Phys. Chem. C. 118 (2014) 8014–8025. doi:10.1021/jp5003947.

[10] R. Bogdanowicz, M. Sawczak, P. Niedzialkowski, P. Zieba, B. Finke, J. Ryl, T. Ossowski, Direct amination of boron-doped diamond by plasma polymerized allylamine film: Direct amination of boron-doped diamond, Phys. Status Solidi A. 211 (2014) 2319–2327. doi:10.1002/pssa.201431242.

[11] H. Li, P. Winget, J.-L. Brédas, Transparent Conducting Oxides of Relevance to Organic Electronics: Electronic Structures of Their Interfaces with Organic Layers, Chem. Mater. 26 (2014) 631–646. doi:10.1021/cm402113k.

[12] M. Zelzer, R. Majani, J.W. Bradley, F.R.A.J. Rose, M.C. Davies, M.R. Alexander, Investigation of cell–surface interactions using chemical gradients formed from plasma polymers, Biomaterials. 29 (2008) 172–184. doi:10.1016/j.biomaterials.2007.09.026.

[13] H.K. Koduru, L. Marino, J. Vallivedu, C.-J. Choi, N. Scaramuzza, Microstructural, wetting, and dielectric properties of plasma polymerized polypyrrole thin films, J. Appl. Polym. Sci. 133 (2016) 43982(1)-43982(10). doi:10.1002/app.43982.

[14] S.H. Brewer, S. Franzen, Optical properties of indium tin oxide and fluorine-doped tin oxide surfaces: correlation of reflectivity, skin depth, and plasmon frequency with conductivity, J. Alloys Compd. 338 (2002) 73–79.

[15] Z. Banyamin, P. Kelly, G. West, J. Boardman, Electrical and Optical Properties of Fluorine Doped Tin Oxide Thin Films Prepared by Magnetron Sputtering, Coatings. 4 (2014) 732–746. doi:10.3390/coatings4040732.

[16] W. Kern, Handbook of semiconductor wafer cleaning technology : science, technology, and applications, Park Ridge, N.J., U.S.A. : Noyes Publications, 1993.

[17] C.O. Kim, S.-Y. Hong, M. Kim, S.-M. Park, J.W. Park, Modification of indium–tin oxide (ITO) glass with aziridine provides a surface of high amine density, J. Colloid Interface Sci. 277 (2004) 499–504. doi:10.1016/j.jcis.2004.04.064.

[18] S.H. Brewer, D.A. Brown, S. Franzen, Formation of Thiolate and Phosphonate Adlayers on Indium- Tin Oxide: Optical and Electronic Characterization, Langmuir. 18 (2002) 6857–6865.




MOST WIEDZY Downloaded from mostwiedzy.pl

[19] M. Terracciano, I. Rea, J. Politi, L. De Stefano, Optical characterization of aminosilane-modified silicon dioxide surface for biosensing, J. Eur. Opt. Soc.-Rapid Publ. 8 (2013).
[20] Pruna R., Palacio F., Martínez M., Blázquez O., Hernández S., Garrido B., López M., Organosilane-functionalization of nanostructured indium tin oxide films, Interface Focus. 6 (2016) 20160056(1)-20160056(8). doi:10.1098/rsfs.2016.0056.
[21] T. Ahuja, Rajesh, D. Kumar, V.K. Tanwar, V. Sharma, N. Singh, A.M. Biradar, An amperometric uric acid biosensor based on Bis[sulfosuccinimidyl] suberate crosslinker/3-aminopropyltriethoxysilane surface modified ITO glass electrode, Thin Solid Films. 519 (2010) 1128–1134. doi:10.1016/j.tsf.2010.08.056.
[22] B. Finke, F. Luethen, K. Schroeder, P. Mueller, C. Bergemann, M. Frant, A. Ohl, B. Nebe, The effect of positively charged plasma polymerization on initial osteoblastic focal adhesion on titanium surfaces, Biomaterials. 28 (2007) 4521–4534. doi:10.1016/j.biomaterials.2007.06.028.
[23] 4.1.3. BUFFER SOLUTIONS, in: Counc. Eur. Eur. Pharmacopoeia, 7.0, Strasbourg, 2007: pp. 489–494.
[24] D.Y. Kwok, T. Gietzelt, K. Grundke, H.-J. Jacobasch, A.W. Neumann, Contact Angle Measurements and Contact Angle Interpretation. 1. Contact Angle Measurements by Axisymmetric Drop Shape Analysis and a Goniometer Sessile Drop Technique, Langmuir. 13 (1997) 2880–2894. doi:10.1021/la9608021.
[25] D.Y. Kwok, A.W. Neumann, Contact angle measurements and interpretation: wetting behavior and solid surface tensions for poly(alkyl methacrylate) polymers, J. Adhes. Sci. Technol. 14 (2000) 719–743. doi:10.1163/156856100742843.
[26] D.Y. Kwok, A.W. Neumann, Contact angle measurement and contact angle interpretation, Adv. Colloid Interface Sci. 81 (1999) 167–249. doi:10.1016/S0001-8686(98)00087-6.
[27] J.J. Iturri Ramos, S. Stahl, R.P. Richter, S.E. Moya, Water Content and Buildup of Poly(diallyldimethylammonium chloride)/Poly(sodium 4-styrenesulfonate) and Poly(allylamine hydrochloride)/Poly(sodium 4-styrenesulfonate) Polyelectrolyte Multilayers Studied by an in Situ Combination of a Quartz Crystal Microbalance with Dissipation Monitoring and Spectroscopic Ellipsometry, Macromolecules. 43 (2010) 9063–9070. doi:10.1021/ma1015984.
[28] H.A. Al-Attar, Q.H. Al-Alawina, A.P. Monkman, Spectroscopic ellipsometry of electrochemically prepared thin film polyaniline, Thin Solid Films. 429 (2003) 286–294. doi:10.1016/S0040-6090(03)00279-7.
[29] J.N. Hilfiker, H.G. Tompkins, Spectroscopic ellipsometry : practical application to thin film characterization, Momentum Press, 2016.
[30] M.E. Orazem, N. Pébère, B. Tribollet, Enhanced Graphical Representation of Electrochemical Impedance Data, J. Electrochem. Soc. 153 (2006) B129–B136. doi:10.1149/1.2168377.
[31] M. Sun, H. Liu, J. Qu, J. Li, Earth-Rich Transition Metal Phosphide for Energy Conversion and Storage, Adv. Energy Mater. 6 (2016) 1600087(1)-1600087(34). doi:10.1002/aenm.201600087.
[32] H. Gerengi, P. Slepski, G. Bereket, Dynamic electrochemical impedance spectroscopy and polarization studies to evaluate the inhibition effect of benzotriazole on copper-manganese-aluminium alloy in artificial seawater, Mater. Corros. 64 (2013) 1024–1031. doi:10.1002/maco.201206565.
[33] J. Ryl, J. Wysocka, M. Cieslik, H. Gerengi, T. Ossowski, S. Krakowiak, P. Niedzialkowski, Understanding the origin of high corrosion inhibition efficiency of bee products towards aluminium alloys in alkaline environments, Electrochimica Acta. 304 (2019) 263–274. doi:10.1016/j.electacta.2019.03.012.
[34] J. Luo, A. Sam, B. Hu, C. DeBruler, X. Wei, W. Wang, T.L. Liu, Unraveling pH dependent cycling stability of ferricyanide/ferrocyanide in redox flow batteries, Nano Energy. 42 (2017) 215–221. doi:10.1016/j.nanoen.2017.10.057.
[35] K.-W. Wu, A. Tedla, Y.-T. Mu, Y. Tai, Interfacial modification of the working electrode of dye-sensitized solar cells to improve the charge transport properties, J. Mater. Chem. A. 1 (2013) 12137–12143. doi:10.1039/c3ta12027a.
[36] S.Y. Heo, J.K. Koh, G. Kang, S.H. Ahn, W.S. Chi, K. Kim, J.H. Kim, Bifunctional Moth-Eye Nanopatterned Dye-Sensitized Solar Cells: Light-Harvesting and Self-Cleaning Effects, Adv. Energy Mater. 4 (2014) 1300632(1)-1300632(7). doi:10.1002/aenm.201300632.

MOST WIEDZY Downloaded from mostwiedzy.pl

[37] X. Wang, X. Wang, Q. Di, H. Zhao, B. Liang, J. Yang, Mutual Effects of Fluorine Dopant and Oxygen Vacancies on Structural and Luminescence Characteristics of F Doped $SnO_2$ Nanoparticles, Materials. 10 (2017) 1398(1)-1398(12). doi:10.3390/ma10121398.
[38] D.R. Deepu, C. Sudha Kartha, K.P. Vijayakumar, How spray rate influences the formation and properties of transparent conducting $SnO_2$ thin films, J. Anal. Appl. Pyrolysis. 121 (2016) 24–28. doi:10.1016/j.jaap.2016.06.013.
[39] P. Baraneedharan, S. Imran Hussain, V.P. Dinesh, C. Siva, P. Biji, M. Sivakumar, Lattice doped Zn–$SnO_2$ nanospheres: A systematic exploration of dopant ion effects on structural, optical, and enhanced gas sensing properties, Appl. Surf. Sci. 357 (2015) 1511–1521. doi:10.1016/j.apsusc.2015.09.257.
[40] J. Wysocka, S. Krakowiak, J. Ryl, Evaluation of citric acid corrosion inhibition efficiency and passivation kinetics for aluminium alloys in alkaline media by means of dynamic impedance monitoring, Electrochimica Acta. 258 (2017) 1463–1475. doi:10.1016/j.electacta.2017.12.017.
[41] D.J. Miller, M.C. Biesinger, N.S. McIntyre, Interactions of $CO_2$ and CO at fractional atmosphere pressures with iron and iron oxide surfaces: one possible mechanism for surface contamination?, Surf. Interface Anal. 33 (2002) 299–305. doi:10.1002/sia.1188.
[42] S. Noel, B. Liberelle, L. Robitaille, G. De Crescenzo, Quantification of Primary Amine Groups Available for Subsequent Biofunctionalization of Polymer Surfaces, Bioconjug. Chem. 22 (2011) 1690–1699. doi:10.1021/bc200259c.
[43] P. Qi, Y. Yang, S. Zhao, J. Wang, X. Li, Q. Tu, Z. Yang, N. Huang, Improvement of corrosion resistance and biocompatibility of biodegradable metallic vascular stent via plasma allylamine polymerized coating, Mater. Des. 96 (2016) 341–349. doi:10.1016/j.matdes.2016.02.039.
[44] C. Winthrop, ed., New Developments in Polylactic Acid Research, UK ed. edition, Nova Science Pub Inc, New York, 2014.
[45] P. Niedziałkowski, T. Ossowski, P. Zięba, A. Cirocka, P. Rochowski, S.J. Pogorzelski, J. Ryl, M. Sobaszek, R. Bogdanowicz, Poly-l-lysine-modified boron-doped diamond electrodes for the amperometric detection of nucleic acid bases, J. Electroanal. Chem. 756 (2015) 84–93. doi:10.1016/j.jelechem.2015.08.006.
[46] A.S. Bondarenko, I.E.L. Stephens, H.A. Hansen, F.J. Pérez-Alonso, V. Tripkovic, T.P. Johansson, J. Rossmeisl, J.K. Nørskov, I. Chorkendorff, The Pt(111)/Electrolyte Interface under Oxygen Reduction Reaction Conditions: An Electrochemical Impedance Spectroscopy Study, Langmuir. 27 (2011) 2058–2066. doi:10.1021/la1042475.
[47] J. Ryl, Ł. Burczyk, A. Zieliński, M. Ficek, A. Franczak, R. Bogdanowicz, K. Darowicki, Heterogeneous oxidation of highly boron-doped diamond electrodes and its influence on the surface distribution of electrochemical activity, Electrochimica Acta. 297 (2019) 1018–1027. doi:10.1016/j.electacta.2018.12.050.
[48] P. Slepski, K. Darowicki, M. Kopczyk, A. Sierczynska, K. Andrearczyk, Electrochemical impedance studies of AB5-type hydrogen storage alloy, J. Power Sources. 195 (2010) 2457–2462. doi:10.1016/j.jpowsour.2009.11.089.
[49] B. Hirschorn, M.E. Orazem, B. Tribollet, V. Vivier, I. Frateur, M. Musiani, Determination of effective capacitance and film thickness from constant-phase-element parameters, Electrochimica Acta. 55 (2010) 6218–6227. doi:10.1016/j.electacta.2009.10.065.
[50] M. Lejeune, F. Brétagnol, G. Ceccone, P. Colpo, F. Rossi, Microstructural evolution of allylamine polymerized plasma films, Surf. Coat. Technol. 200 (2006) 5902–5907. doi:10.1016/j.surfcoat.2005.09.003.
[51] M. Elzbieciak, M. Kolasińska, S. Zapotoczny, R. Krastev, M. Nowakowska, P. Warszyński, Nonlinear growth of multilayer films formed from weak polyelectrolytes, Colloids Surf. Physicochem. Eng. Asp. 343 (2009) 89–95. doi:10.1016/j.colsurfa.2009.01.034.
[52] J.B. Schlenoff, S.T. Dubas, Mechanism of Polyelectrolyte Multilayer Growth: Charge Overcompensation and Distribution, Macromolecules. 34 (2001) 592–598. doi:10.1021/ma0003093.

MOST WIEDZY Downloaded from mostwiedzy.pl